Cellulose (2021) 28:11051–11066
https://doi.org/10.1007/s10570-021-04192-z

ORIGINAL RESEARCH

Sequential assembly of PEDOT/$BiVO_4$/FeOOH onto cotton fabrics for photocatalytic degradation of reactive dyes

Benxian Yu · Narendra Reddy · Baojiang Liu · Zhijia Zhu · Wei Wang · Chunyan Hu

Received: 17 May 2021 / Accepted: 13 September 2021 / Published online: 27 September 2021

Abstract This paper demonstrates that a multilayered absorbent developed using Poly(3,4-ethylenedioxythiophene) (PEDOT) modified cotton fabrics provides excellent photocatalytic degradation and remove dyes in wastewater. Low cost, highly efficient and biobased sorbents for removing dyes and other pollutants in wastewater are desirable. However, there are very few absorbents that meet these criteria. Bismuth vanadate ($BiVO_4$) is a unique material with strong visible light absorption and valence band potential suitable for the degradation of dyes. However, the photogenerated carriers of single $BiVO_4$ get recombined easily, and it is difficult to recover the powder which may cause secondary pollution. To overcome this limitation, we have successfully prepared a composite containing PEDOT/$BiVO_4$/Iron oxide hydroxide (FeOOH) on cotton fabrics in a simple two-step process. Initially, cotton fabrics were treated with PEDOT and later $BiVO_4$/FeOOH onto the modified fabrics. When the cotton-based composite was used as sorbent for reactive brilliant blue dye (RB-19), a high degradation level of 95.6% was possible within 2 h under visible light. Further, the sorbent had high recyclability of 92.3% even after 5 sorption and desorption cycles. The experiment suggests that the presence of h^+ and ·OH free radicals along with excellent electron-hole transport properties of PEDOT were responsible for the high level of degradation.

B. Yu · B. Liu · Z. Zhu · W. Wang · C. Hu (✉)
Key Lab of Science and Technology of Eco-textile, Ministry of Education, College of Chemistry, Chemical Engineering and Biotechnology, Innovation Center for Textile Science and Technology, Donghua University, No. 2999 North Renmin Road, Shanghai 201620, China
e-mail: chunyanhu@dhu.edu.cn

N. Reddy
Centre for Incubation, Innovation, Research and Consultancy (CIIRC), Jyothy Institute of Technology, Thataguni, Off Kanakapura Road, Bangalore, Karnataka 560082, India

W. Wang
Department of Textile & Garment Engineering, Changshu Institute of Technology, Suzhou 215500, China

Graphic abstract

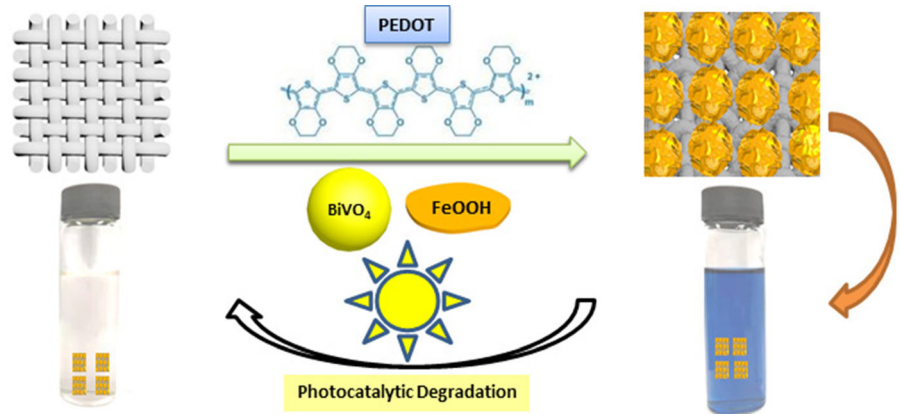

Keywords $BiVO_4$ · Photocatalytic cotton · p-n heterojunction · Reactive dye degradation

Introduction

Manufacturing industries and, more specifically, textiles, pharmaceuticals and metal processing units use high energy and resource- intensive levels and contribute significantly to industrial pollution (El-Hout et al. 2020; Kumar et al. 2020; Zhang et al. 2020a). Several approaches are used to reduce and treat industrial pollution. Among the various pollution treatment techniques, adsorption purification (Sun et al. 2020), biodegradation (Liu et al. 2020), Fenton oxidation (Guo et al. 2020), etc., have been commonly adopted. However, these treatments are expensive, are energy- intensive and in many cases cause secondary pollution. Dyes produced in textile processing units, released into water, are a significant and major cause of pollution. Despite considerable efforts to develop technologies to reduce and treat dyeing waste water, there are no economically viable techniques suitable for adoption on a large scale. For instance, plenty of biobased sorbents have shown potential to remove dyes from waste water on a laboratory scale but such absorbents' large-scale availability and cost limit their practical use (Duan et al. 2019; Srinivasan and Viraraghavan 2010). Recently, nanomaterials and advanced oxidation processes that provide higher efficiency and lower cost than conventional techniques have been developed (Samadi et al. 2019).

Oxidation processes to treat dyes and organic pollutants are classified as heterogenous photocatalysis or homogenous oxidation processes. Compared to the two methods, the photocatalytic degradation of dyes and organic pollutants is an emerging and promising technology to treat polluted water. Photocatalytic degradation is considerably less expensive, efficient, has high catalytic activity, and is adaptable on a large scale. Hence, both organic and inorganic photocatalytic materials have been developed and extensively studied to remove pollutants (Lum et al. 2020; Marimuthu et al. 2020; Samadi et al. 2019). Studies have demonstrated that semiconductor-based nanostructures are particularly suited for photocatalytic degradation. For example, Tushar Kanti Das et al. (2020) prepared Ag/poly(norepinephrine)/MnO_2 nanocatalyst and showed high reduction of 4-nitrophenol and 4-nitroaniline within 540 min. Similarly, Sanjay Remanan and co-workers synthesized MoS_2 nanosheets decorated poly(vinylidene fluoride) (PVDF) sponges with excellent antibacterial activity against *Escherichia coli* (*E. coli*) (Remanan et al. 2020). Tushar Kanti Das et al. (2021) prepared sliver nanoparticles on the surface of poly(epinephrine) coated CeO_2 nanotubes with high catalytic activity to 4-nitrophenol and methylene blue. These materials excite electrons in the conduction band and create holes in the valence band. Further, the electron-hole (e^--h^+) pairs generate various oxygenated radical species capable of photocatalytic dye degradation.

The type of material and conditions used for photocatalytic degradation determine the extent of the removal of pollutants. For example, TiO_2 is an

excellent photocatalyst with high stability and limited toxicity. However, TiO_2 has a large band gap (3.4 eV) resulting in poor activity in the visible light range. Hence, valence band electrons in TiO_2 can be excited only in ultraviolet light (Hu et al. 2020). Therefore, considerable research is being done to improve the photocatalytic activity of materials in the visible light range.

Photocatalytic materials such as bismuth vanadate ($BiVO_4$) has received widespread attention as a biosorbent due to its high visible light utilization, non-toxicity, suitable energy band position and stable crystal structure. Generally, $BiVO_4$ has three different crystal structures, including monoclinic crystal (a = 5.1935Å, b = 5.0898Å, c = 11.6972Å), scheelite tetragonal crystal (a = b = 5.1470Å, c = 11.7216Å) and zircon ore tetragonal crystal (a = b = 7.303Å, c = 6.584Å) (Ikeda et al. 2018; Laraib et al. 2019). Among them, the monoclinic $BiVO_4$ has a higher photocatalytic performance, separation efficiency of photo-generated electrons and holes due to a built-in electric field (Park et al. 2013). The valence band position of $BiVO_4$ is about + 2.4 ev (vs. NHE), which is more positive than $OH^-/\cdot OH$ + 1.89ev (vs. NHE) (Wang et al. 2020b; Yang et al. 2021). Theoretically, it is easy to generate ·OH radicals with strong oxidizing ability by photocatalysis, which can oxidatively degrade most organic pollutants. Therefore, $BiVO_4$ is an ideal material with substantial potential for photocatalytic removal of organic or inorganic pollutants. However, using $BiVO_4$ individually has drawbacks, such as higher recombination of photogenerated electron-hole pairs, lower visible light utilization, and difficulty in recycling (Yan et al. 2020; Zhang et al. 2019a). Researchers have attempted to overcome this limitation by controlling the morphology, heterojunction interface and developing composites of $BiVO_4$ by modulating the reaction synthesis conditions. For instance, changing the shape and size of the photocatalytic material modifies the material's interfacial energy, charge transport and optical performance, thereby improving the photocatalytic activity. Liu and co-workers proved that 1D nano $BiVO_4$ has a shorter radial transmission distance and hence can efficiently separate photogenerated carriers exhibiting high catalytic activity (Liu et al. 2014).

Also, construction of a heterojunctions between $BiVO_4$ and another semiconductor photocatalytic materials such as $CuO/BiVO_4$ (Ran et al. 2019), $ZnIn_2S_4/BiVO_4$ (Yuan et al. 2020), $WO_3/BiVO_4$ (Coelho et al. 2020), etc. are capable of separating photogenerated electron-hole pairs. In the heterostructures, the electrons and holes generated by light excitation are transferred to the conduction band and valence band of different semiconductors respectively. Such transfer greatly reduces the chance of recombination of photogenerated electrons and holes. In addition, reduced graphene oxide (r-GO), carbon nanotube, Polypyrrole (PPy) and other carbon materials with excellent electrical conductivity can be combined with $BiVO_4$ to improve the electron transport performance. This facilitates the separation of photogenerated electron holes (Wang et al. 2020a; Yan et al. 2020).

In addition to increasing the absorption of pollutants, it is also important that the material used for removal of the pollutants should be biodegradable and easily recyclable. Since many photocatalysts are in powder form, it becomes difficult to recover and reuse them. To overcome this limitation, researchers have developed techniques such as addition of photocatalyst particles (Ji et al. 2020), increasing the magnetic properties of the photocatalyst powder (Almeida et al. 2020) or synthesize the photocatalyst onto PET-ITO substrate (Yu et al. 2017). The above methods still have shortcomings, such as insufficient mechanical strength, high cost, and complicated procedures but ensures recovery of the photocatalyst. Cotton fabric has the obvious advantages of low cost, strong mechanical property, and good flexibility, to be an ideal photocatalyst loading template. A few articles have suggested the use of cotton fabric as support for photocatalysts since cotton fabrics are easily recyclable (Ran et al. 2019; Yan et al. 2020; Zhang et al. 2019a).

The common metal hydroxide FeOOH can function as a co-catalyst and is considered to be an excellent photosensitive material for inhibiting electron-hole recombination. For example, gC_3N_4-Fe_3O_4/β-FeOOH (He et al. 2020), $FeOOH/Bi_2MoO_6$ (Hu et al. 2020), and $FeOOH/TiO_2/BiVO_4$ (Yin et al. 2019) composite catalysts have exhibited enhanced photocatalytic performance. FeOOH and other semiconductor photocatalysts combine well to form a typical composite heterojunction, thereby improving the light absorption capacity of the sample. Such combinations can also accelerate the interface charge transfer capacity and

hence, reduce the frequency of addition of photogenerated carriers.

In addition to formation of the heterojunctions, adding conductive polymers with good electron mobility to the photocatalysts to form a ternary composite is also an effective way to enhance photocatalytic performance. Poly(3,4-ethylenedioxythiophene) (PEDOT) is one of the conductive polymers that has been widely studied due to its excellent electrical conductivity, biocompatibility, and flexibility. Studies have shown that poly(3,4-ethylenedioxythiophene) (PEDOT) has ultra-high electrical conductivity particularly during photoluminescence. It is usually used as a hole transport layer to quickly transfer photo-generated holes and inhibit the Auger recombination of electrons and holes (Ivanko et al. 2019; Koyama et al. 2015). PEDOT has a wide range of applications in electromagnetic shielding, biomass sensors, light-emitting diodes, and other fields (Ghosh et al. 2019; Gueye et al. 2020; Kayser and Lipomi 2019). PEDOT is an organic semiconductor that can combine with inorganic semiconductor and form an organic-inorganic hybrid composite structure to obtain enhanced photochemical properties (Trzciński et al. 2016; Zhang et al. 2020b). Cellulose-based composite photocatalytic materials usually have low carrier mobility due to their low conductivity, resulting in poor photocatalytic reaction kinetics. We have utilized PEDOT as electrons and holes transport layer in our sequentially assembled composite fabric. PEDOT has affinity with cotton fabric (Ghosh et al. 2019), excellent electron hole transport properties as well as easily recombines with inorganic semiconductors (Wang et al. 2018).

In this paper, we use a simple dipping and drying method to assemble PEDOT on a clean cotton fabric to improve its electrical conductivity. Later, the pre-prepared $BiVO_4$ was loaded on the modified cotton fabric by immersion at high temperature. Through this approach, FeOOH is synthesized on the fabric through a mild hydrothermal reaction. The obtained PEDOT/$BiVO_4$/FeOOH@Cotton demonstrated excellent photocatalytic performance in the organic dye removal experiment. In the subsequent experiments, the prepared composite material exhibited good stability. The photocatalytic mechanism of PEDOT/$BiVO_4$/FeOOH@cotton hybrid was studied through free radical and hole scavenging experiments. A possible mechanism for improving the photocatalytic activity of $BiVO_4$ has also been proposed.

Materials and methods

Materials

PEDOT: PSS aqueous suspension (Clevious pH1000) was purchased from Heraeus Electronic Materials Co., Ltd. Bismuth nitrate pentahydrate ($Bi(NO_3)_3{\cdot}5H_2O$, $\geq$ 99%), ammonium metavanadate (NH_4VO_3, $\geq$ 99.0%), ferric chloride hexahydrate ($FeCl_3{\cdot}6H_2O$), absolute ethanol (CH_3CH_2OH), urea ($CO(NH_2)_2$, $\geq$ 99%) were purchased from Sinopharm Chemical Reagent Co., Ltd. Cotton fabric (plain, 120 g/m^2) was purchased from Esquel Group, China. The cotton fabric was ultrasonically cleaned with 100 mL of distilled water and ethanol mixture (1:1) for 30 min before use. Sodium oxalate (Na-OA), t-butanol (TBA) and 1,4-p-benzoquinone (BQ) were obtained from Adamas Reagent Co., Ltd. Reactive dyes (RB-19) were purchased from Dystar Printing and Dyeing Technology Co., Ltd. All these reagents were of analytical grade and used without further purification.

Modification of cotton fabric

The cleaned cotton fabric was first treated with PEDOT through a simple dip drying method. The detailed steps are as follows. First, 2 mL of PEDOT: PSS solution was added into 50 mL of absolute ethanol, sonicated for 15 min at room temperature to form a uniform solution. Cleaned cotton fabrics weighing 0.4 g (5 × 5 cm) were immersed in this solution and heated at 60 °C for 15 min. This process was repeated five times to obtain a uniform coating of PEDOT on the cotton fabrics.

Assembly of $BiVO_4$/FeOOH catalyst

The single $BiVO_4$ catalyst was prepared by a typical hydrothermal reaction (Wang et al. 2020b). First, 5 mmol $Bi(NO_3)_3{\cdot}5H_2O$ and NH_4VO_3 was dissolved in 20 mL of 4 M nitric acid and sodium hydroxide, respectively, and then ultrasonically treated for 15 min. Next, under magnetic stirring, the $Bi(NO_3)_3{\cdot}5H_2O$ solution was added drop-wise into the NH_4VO_3 solution to form a yellow suspension and

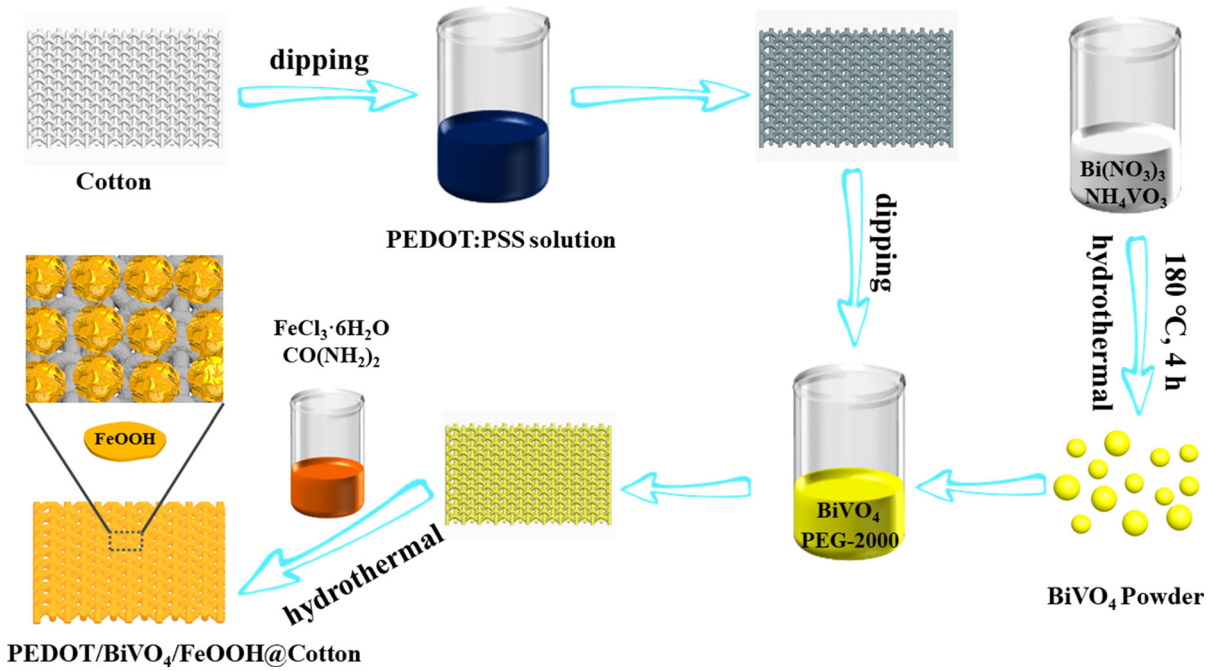

Fig. 1 Illustration of manufacturing process of PEDOT/$BiVO_4$/FeOOH@Cotton composite

subsequently, the pH of the solution was reduced to 3. The solution was maintained for 30 min before the hydrothermal treatment was done in an oven at 180 °C for 4 h. Finally, after cooling to room temperature, the prepared $BiVO_4$ was washed with ethanol and water several times and further dried to obtain a single $BiVO_4$ catalyst.

To form the composite on the cotton fabrics, 0.1 g $BiVO_4$ and 0.01 g PEG-2000 were uniformly dispersed in 50 ml deionized water into which the PEDOT treated cotton was added and the temperature of the suspension was raised to 98 °C. PEG-2000 was used as a dispersing agent for suspending $BiVO_4$ particles in the medium. The excellent adhesiveness of PEG-2000 helps achieve high adhesion of $BiVO_4$ to cellulose. The fabric was maintained in the water bath at 98 °C for 60 min. Later, the fabric was taken out and dried in an oven at 60 °C.

Based on the successful incorporation of PEDOT/$BiVO_4$ onto the cotton fabrics, deposition of an additional layer of FeOOH was considered. To add FeOOH, a (Xue et al. 2019) gentle hydrothermal method was followed. Initially, 0.013 g of $FeCl_3{\cdot}6H_2O$ and 0.003 g of urea ($CO(NH_2)_2$) were dissolved in 100 mL of deionized water to obtain a uniform solution. Later, the prepared PEDOT/$BiVO_4$@Cotton fabric was added and the hydrothermal reaction was carried out at 100 °C for 4 h. The treated fabric was thoroughly washed with deionized water and dried to obtain the multifunctional PEDOT/$BiVO_4$/FeOOH@Cotton composite material. The lower hydrothermal reaction temperature and longer reaction time allows FeOOH to grow uniformly, with minimal damage to the strength of the cotton fabrics during the hydrothermal reaction. The complete step-by-step process of manufacturing the PEDOT/$BiVO_4$/FeOOH@Cotton composite is shown in Fig. 1.

Analysis of fabrics

The crystal structure of the composite photocatalytic material was analyzed by an X-ray polycrystalline diffractometer (D/max-2550 PC) under Cu-Kα radiation. The 2θ range was from 5° to 90° with scanning speed of 0.02°/0.06 s. The morphology and size of the composite material were observed by scanning electron microscope (SEM: JSM-5600LV). The content and distribution of the elements on the surface of the composite were analyzed using energy dispersive spectrometer (EDS: IE 300 X). X-ray photoelectron spectrometer (XPS: Escalab 250Xi) was used to

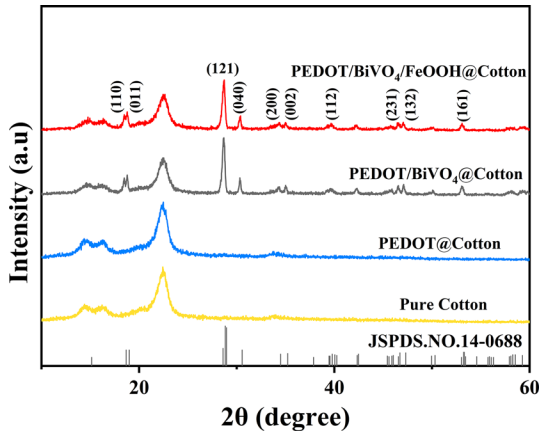

Fig. 2 XRD patterns of pure Cotton, PEDOT@Cotton, PEDOT/$BiVO_4$@Cotton and PEDOT/$BiVO_4$/FeOOH@Cotton

analyze the surface states of the valence elements on the photocatalytic fabrics by measuring the light absorption of the photocatalytic fabric between 200 and 800 nm in an ultraviolet-visible spectrometer (UV-vis: UV-3600) with $BaSO_4$ as a reference.

Photodegradation of reactive dye

The ability of the cotton composite for photocatalytic removal of reactive brilliant blue dye (RB-19) was investigated. In this study, the treated fabric (5 × 5 cm; 0.40 g) was added into 50 mL of 60 mg/L RB-19 solution in a quartz tube. The quartz tube was placed in the photochemical reactor, and a 1000 W Xenon lamp radiant tube was used to simulate sunlight. First, under dark conditions, the fabric immersed in the dye solution was magnetically stirred for 30 min to reach the dye adsorption-desorption equilibrium. Later, the light source was activated for 2 h to start the photocatalytic reaction. During this period, precisely 5 mL solution was taken out every 30 min and the absorbance was measured in an ultraviolet spectrophotometer (model U3310). To eliminate the influence of other factors during the photoreaction process, a cold-water circulation system was used to maintain he temperature inside the photochemical reactor at about 25 °C.

To explore the possible mechanism of photocatalytic fabric removal of dyes, free radical scavengers (Na-OA, t-BuOH, BQ) were added. The photochemical reaction was carried out for 2 h, and the changes in dye degradation rate were used to determine the main active species responsible for the photoreaction. After each cycle of exposure and dye degradation, the fabric was soaked in deionized water for 3 h to clean it and then dried in an oven at 60 °C. Treated fabrics were reused and subjected to the dye absorption and photocatalytic degradation for five cycles.

Results and discussion

Changes in the physical structure of the cotton fabrics

Figure 2 shows the changes in the X-ray diffraction patterns of pure cotton and cotton fabrics after various modifications using photodegradation chemicals. In addition to the distinct diffraction peaks of pure cotton fabrics (main peak at 22.7° belonging to the (200) plane), it is clearly observed that the diffraction peaks of the composite sample coincide with the $BiVO_4$ monoclinic phase (JCPDS.NO.14-0688). Since PEDOT is an amorphous substance, PEDOT treated cotton fabrics do not show any major changes in the diffraction peaks compared to unmodified cotton fabrics (Zhang et al. 2020b). Similarly, the diffraction peaks of FeOOH are also not observed, probably due to their low concentration on the fabrics (Shi et al. 2020). No other impurity peaks were observed, indicating that the prepared sample was comparatively pure. From the comparison of the diffraction peaks of PEDOT/$BiVO_4$@Cotton and PEDOT/$BiVO_4$/FeOOH@Cotton, it can be inferred that the hydrothermal reaction after loading $BiVO_4$ did not affect the crystal structure of $BiVO_4$ suggesting that $BiVO_4$ could withstand the conditions due to the hydrothermal reaction.

FE-SEM images provide information on the distribution and structural changes of the photocatalytic material on the fabric surface during the preparation process. Figure 3, shows that the surface of untreated cotton fabrics is smooth and clean (Fig. 3a, e). Compared to the untreated cotton fabric, the surface of the PEDOT@Cotton (Fig. 3b, f) is covered with a uniform thin layer, implying that PEDOT has been successfully loaded onto the surface of cotton fabric after the dipping and drying steps. This change is caused because the conductive polymer PEDOT macromolecular chains have many polar groups, such as ether bonds. These form hydrogen bonds with the

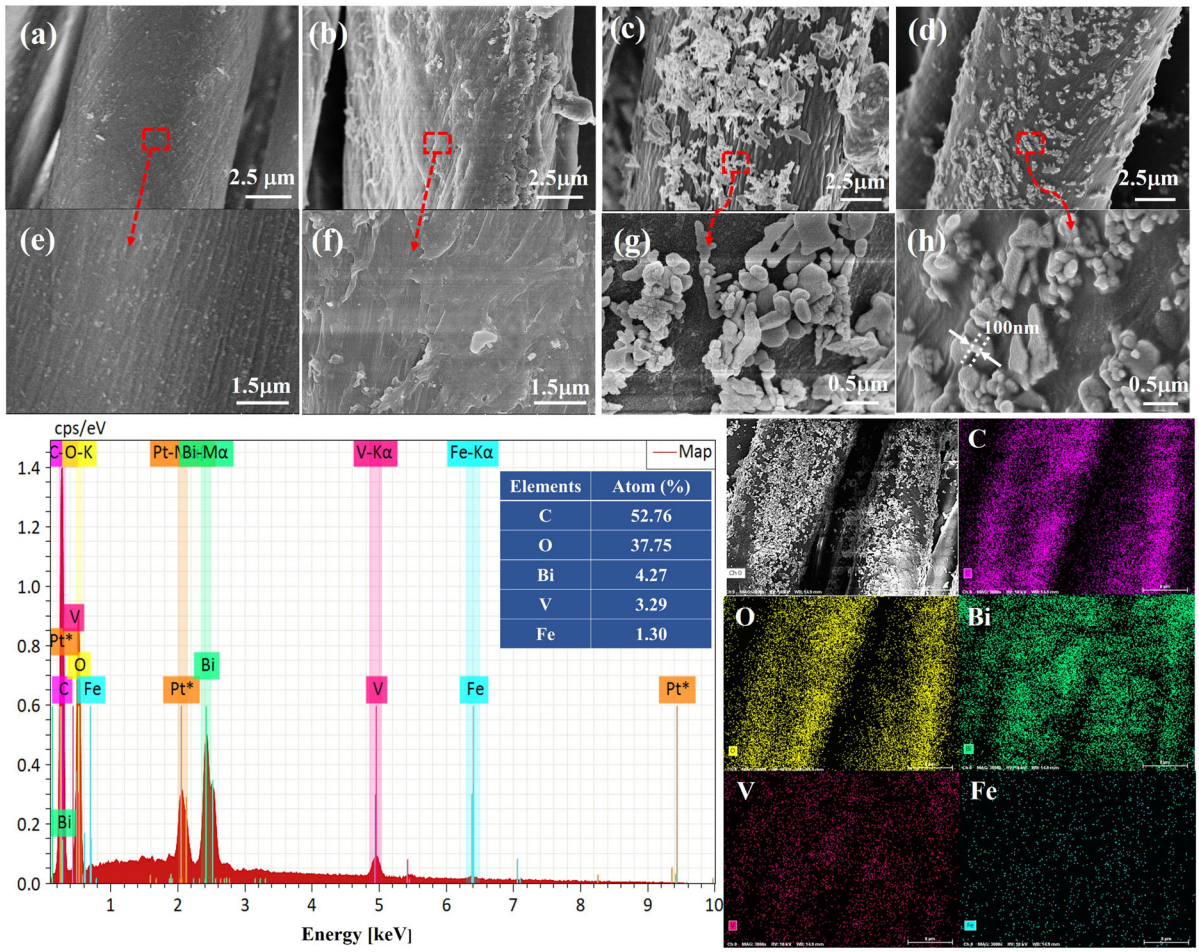

Fig. 3 FE-SEM images of Clean Cotton (**a**, **e**), PEDOT@Cotton (**b**, **f**), PEDOT/$BiVO_4$@Cotton (**c**, **g**), PEDOT/$BiVO_4$/FeOOH@Cotton (**d**, **h**) and EDS-mapping of PEDOT/$BiVO_4$/FeOOH@Cotton

hydroxyl groups on the cellulose (Ghosh et al. 2019). From the FE-SEM images of PEDOT/$BiVO_4$@Cotton (Fig. 3c, g), it can be observed that the $BiVO_4$ crystals deposited on the cotton fabrics are in the form of flakes and plates which are uniformly dispersed on the surface of the fibers. In addition, the magnified Fig. 3g shows that the $BiVO_4$ flakes have size between 200 and 300 nm. The flaky structure is more evident after using the PEDOT/$BiVO_4$@Cotton as a template to synthesize FeOOH by hydrothermal reaction (Fig. 3d, h). In the magnified image Fig. 3h, we can observe that the particle's size is about 100 nm. The above results demonstrate the successful deposition of PEDOT/$BiVO_4$/FeOOH@Cotton composite photocatalytic fabric.

From the EDS spectrum, it can be observed that the five elements C, O, Bi, Fe and V form a major portion of the fabric complex. Among them, the atomic content of C and O elements is the highest since the cotton fabric and PEDOT are organic materials. The atomic percentages of Bi and V are in good agreement with the stoichiometric ratio of $BiVO_4$ and cotton fabric used. The proportion of the Fe element is the lowest because the FeOOH content is low, as observed in the XRD patterns.

The elemental composition and chemical valence state of the composite photocatalytic fabric samples were characterized by XPS. As seen in Fig. 4a, the XPS spectrum indicates that Bi, C, V, O, and Fe elements exist in PEDOT/$BiVO_4$/FeOOH@Cotton fabric. The high-resolution XPS spectrum in

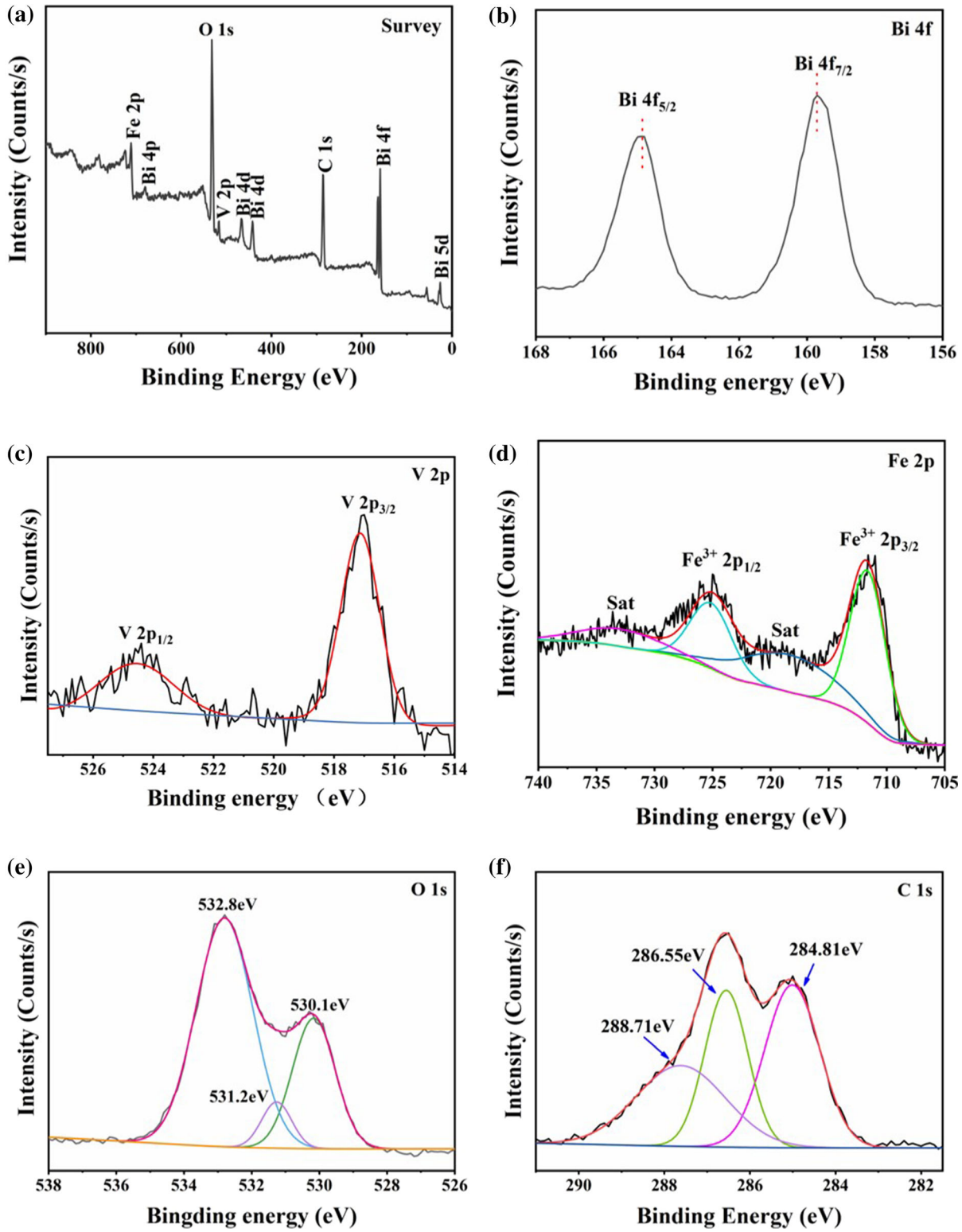

Fig. 4 XPS spectrum of PEDOT/$BiVO_4$/FeOOH@Cotton composite **a** full survey, high-resolution XPS spectrum of **b** Bi 4f, **c** V 2p, **d** Fe 2p, **e** O 1s and **f** C 1s

Fig. 4b–f shows that the binding energies at 157.4 eV and 164.8 eV can be attributed to Bi $4f_{5/2}$ and Bi $4f_{7/2}$ in $BiVO_4$, respectively, which confirm that Bi exists as Bi^{3+} (Shen et al. 2020; Soomro et al. 2020). As seen from Fig. 4c, the binding energy at 516.9 eV and 524.4 eV corresponds to V $2p_{3/2}$ and V $2p_{1/2}$, respectively, which matches well with V^{5+} belonging to VO_4^{3-} (Ju et al. 2020). This result indicates the presence of $BiVO_4$ in the composite photocatalytic fabric. Figure 4d shows the high-resolution XPS spectrum of Fe 2p with a binding energy of 711.6 eV and 725.3 eV assigned to Fe $2p_{3/2}$ and Fe $2p_{1/2}$, respectively, indicating that the Fe element in the photocatalytic fabric is Fe^{3+} (She et al. 2020). At the same time, the high-resolution XPS spectrum of O 1s (Fig. 4e) shows two peaks with binding energies of 531.2 and 532.8 eV that can be assigned to Fe-O and Fe-OH bonds (Zhang et al. 2019a), which confirms that FeOOH was successfully formed during the hydrothermal reaction. The peak at 530.1 eV is attributed to the lattice oxygen in the crystal $BiVO_4$ (Gao et al. 2020). Besides, the XPS spectrum of C 1 s has three peaks at a binding energy of 284.8 eV, 286.5 eV and 288.7 eV corresponding to the –C–C, –C–O, and –C=O functional groups in the fabric (Wang et al. 2020a).

The optical absorption of the prepared photocatalytic composite fabrics was studied by UV-vis diffuse absorption spectra. As seen from Fig. 5a, the intensity of absorption of the pure cotton fabric was considerably low and in the range of 200–800 nm and did not increase significantly even after treating with PEDOT. However, the optical absorption of photocatalytic fabrics has been significantly enhanced, especially in the 200–450 nm wavelength region after treatment with $BiVO_4$. Further increase in the optical intensity can be observed after treating with FeOOH. It is worth noting that the enhancement of visible light absorption above 400 nm is of great significance to improve the utilization of light energy. This phenomenon can be attributed to the optical properties of FeOOH, which improve the visible light absorption of $BiVO_4$.

The Kubelka–Munk equation was used to estimate the band gap (Eg): $(\alpha hv)^2 = (Ahv\text{-}Eg)$, where α, h, v, A and Eg represent the absorption coefficient of diffuse reflection, Planck's constant, vibration frequency, proportional constant, and band gap respectively (Zhang et al. 2019a). As shown in Fig. 5b, the band gap of PEDOT/$BiVO_4$@Cotton is 2.44 eV while the band gap of PEDOT/$BiVO_4$/FeOOH@Cotton sample is approximate 2.30 eV. This shows that FeOOH reduces the band gap of $BiVO_4$, which means that it has a better light utilization rate, enhancing the photocatalytic performance.

Typically, the separation efficiency of photoexcited electrons and holes can be characterized by Photoluminescence Spectroscopy (PL). The stronger PL peaks mean a higher recombination rate of electron-hole pairs and lower separation efficiency. In the above discussion, it has been shown that PEDOT/$BiVO_4$@-Cotton and PEDOT/$BiVO_4$/FeOOH@Cotton have significant light absorption. The electron-hole

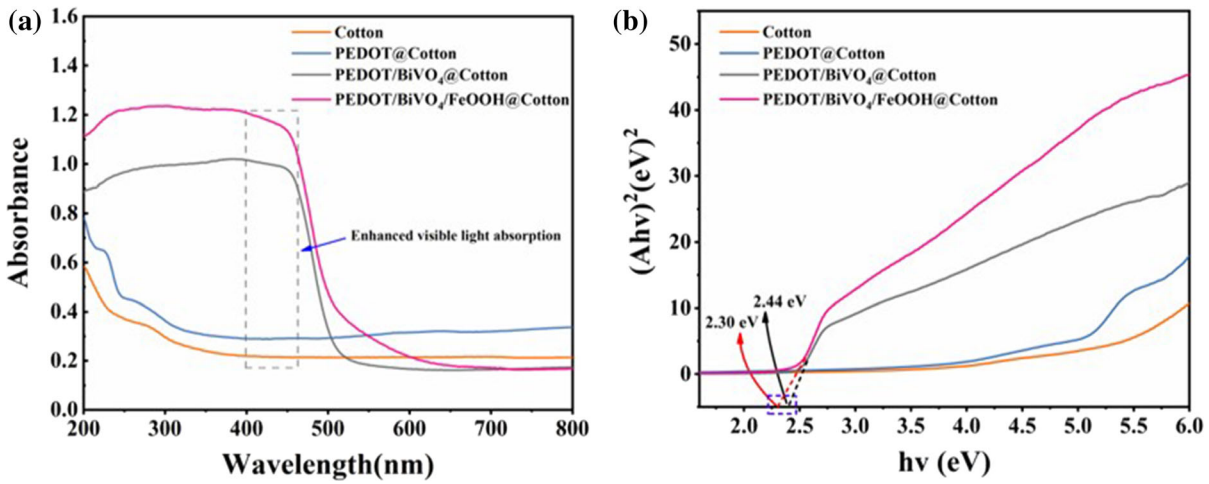

Fig. 5 UV–Vis diffuse reflectance spectra of untreated and treated fabrics (**a**) and the corresponding plots of $(\alpha hv)^2$ versus hv (**b**)

separation efficiency of the treated fabrics was determined using PL studies. The PL characterization results in Fig. 6a show that the PEDOT/$BiVO_4$/FeOOH@Cotton fabric peak is much lower than PEDOT/$BiVO_4$@Cotton suggesting that the introduction of FeOOH enhances the separation of photoexcited pairs.

To further understand the separation efficiency of photoexcited carriers during the process of photocatalysis, we performed the photocurrent analysis on the two photocatalytic fabrics. As shown in Fig. 6b, the intensity of the transient photocurrent was detected after switching the lights every 50 s. A stable transient photocurrent can be observed in both samples in each cycle. Among them, PEDOT/$BiVO_4$/FeOOH@Cotton exhibits a stronger transient photocurrent, indicating that it has a higher light-excited carrier density and a higher separation efficiency. This result is consistent with the photoluminescence spectrum results. Based on the above observations, it can be inferred that FeOOH forms a heterostructure with $BiVO_4$, which changes the transfer path of photoexcited electrons and holes, and significantly improves their separation efficiency.

Photocatalytic results of samples

In this study, we have evaluated the photocatalytic performance of untreated and treated cotton by degrading a common reactive dye (RB-19). To account for the light stability of the dye, we first irradiated the dye for 2 h without adding a catalyst and found that the dye concentration barely decreased confirming that the photostability of the substrate has little effect on the experimental results.

As seen from Fig. 7a, the concentration of dyes in the solution starts to decrease after 15 min, and after 30 min, the sorption reaches saturation. Among the different fabrics used, the sorption increases as the layers on the cotton fabric increase. The dye adsorption performance of these composite materials can be attributed to the porosity of the cotton substrate and its high affinity for reactive dyes (Fan et al. 2019) and to increased specific surface area of the composite materials (Yang et al. 2020). Figure 7b shows that the reaction time of 2 h in simulated sunlight did not provide the cotton fabric and PEDOT@Cotton fabric ability to degrade RB-19 significantly. However, modification of the fabrics with $BiVO_4$ increases the dye absorption to 64.8%. It is hypothesized that this phenomenon is mainly due to the weak light absorption properties of cotton and PEDOT, while $BiVO_4$ has considerable light-driven performance (Yentür and Dükkancı 2020). Although PEDOT/$BiVO_4$@Cotton has a band gap of 2.44 eV and visible light driving characteristics, the rapid recombination of photoexcited carriers and limited light absorption may severely hinder photocatalytic activity. The PEDOT/$BiVO_4$/FeOOH@Cotton sample exhibits the best photocatalytic performance compared to other samples. The photocatalytic degradation of more than 95% of the reactive dyes occurs within 2 h. This may be

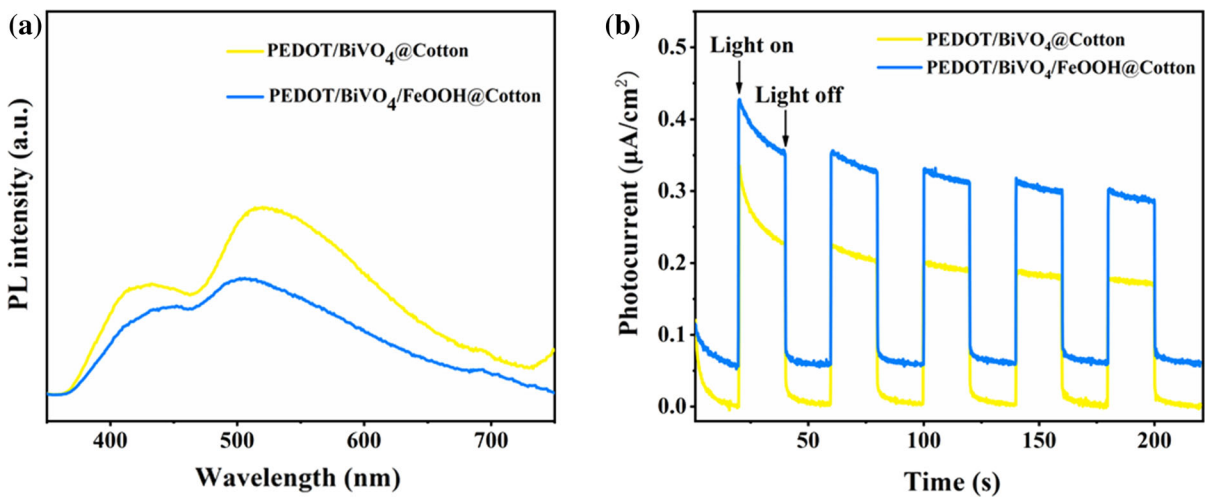

Fig. 6 PL characterization results of photocatalytic fabrics with enhanced light absorption (**a**) and transient photocurrent results (**b**)

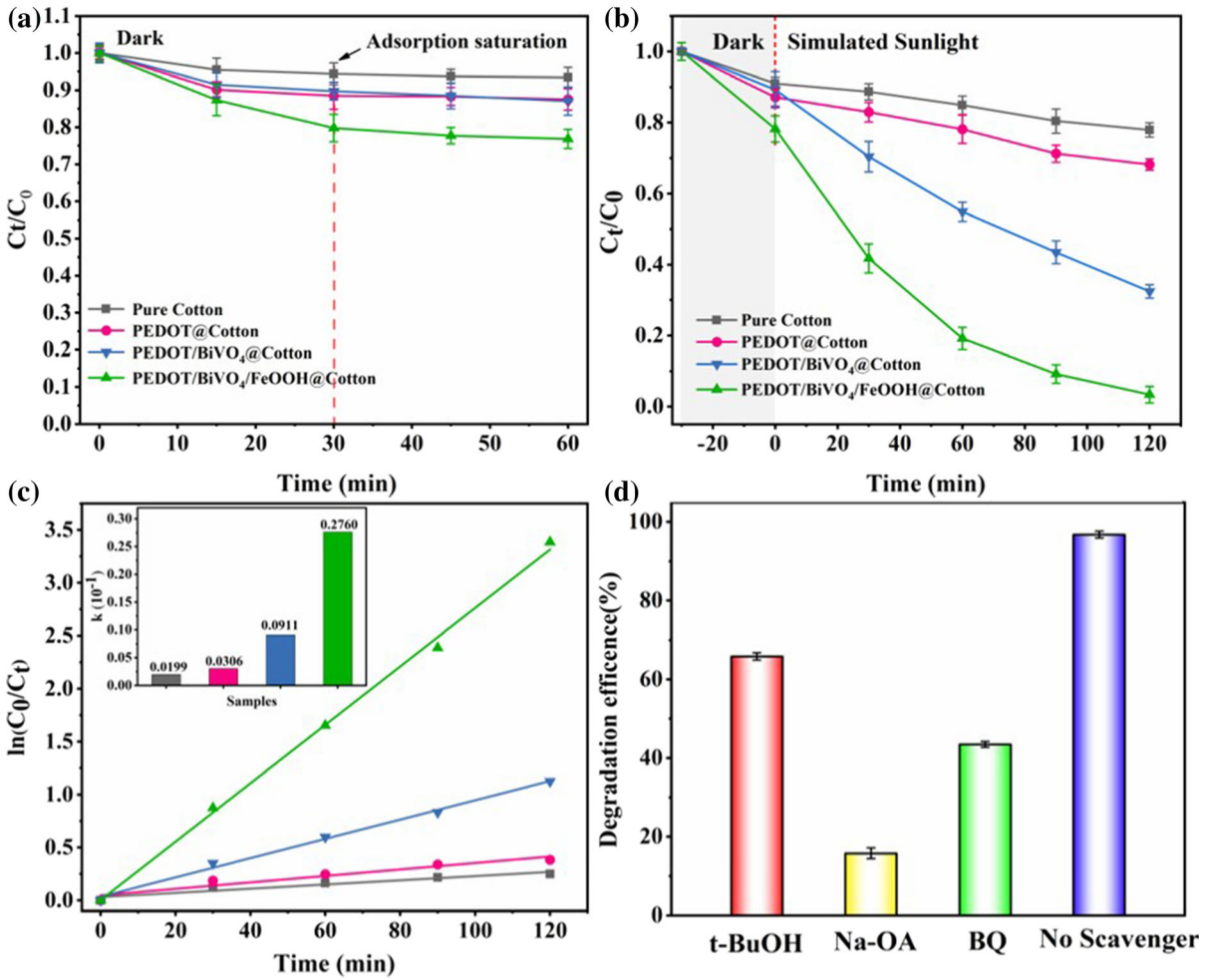

Fig. 7 The dye adsorption curves (**a**), the dye concentration in photocatalytic degradation process (**b**), the first-order model fitting straight line (**c**) and the dye degradation results of radical capture experiment (**d**) of all samples

because FeOOH and $BiVO_4$ have good energy band matching to form a p-n heterojunction, which promotes the separation of light-excited holes and electrons, thereby significantly improving the photocatalytic performance.

Further, the dye degradation kinetics were assigned to the apparent first-order model: $\ln(C_0/C_t) = kt$. Where C_0, C_t, k, and t represent the initial dye concentration, the dye concentration at time t, the reaction rate constant and time, respectively. The results after linear fitting are shown in Fig. 7c, and it can be clearly observed that the $\ln(C_0/Ct) \sim t$ point has good linearity. The dye degradation reaction rate constant k can be measured from the slope of the fitted straight line. The k of pure Cotton, PEDOT@Cotton, PEDOT/$BiVO_4$@Cotton and PEDOT/$BiVO_4$/FeOOH@Cotton are 0.00199 min^{-1}, 0.00306 min^{-1}, 0.00911 min^{-1} and 0.02760 min^{-1}, respectively. The reaction rate constant of PEDOT/$BiVO_4$/FeOOH@Cotton is much higher than that of other samples, and its value is more than 3 times that of PEDOT/$BiVO_4$@Cotton suggesting that the treated fabric has fast dye photodegradation, consistent with the results discussed before.

Possible photodegradation mechanism

The main oxidizing species in the photocatalytic oxidation reaction are light-excited holes h^+, radicals $\cdot O_2^-$ and ·OH. The paper proves the successful preparation of PEDOT/$BiVO_4$/FeOOH@Cotton composite photocatalysis and its superior

photodegradation performance. To better understand the possible mechanism of the photocatalytic degradation of dyes, the hole scavenger sodium oxalate (Na-OA), the free radical $\cdot O_2^-$ scavenger benzoquinone (BQ) and the free radical ·OH scavenger t-butanol (t-BuOH) were added to the dye solution. As a control, a photodegradation experiment without adding any scavenger agents was carried out under the same conditions. It can be observed from Fig. 7d, that in the experiment without adding scavengers, the degradation rate reached more than 96% after 2 h. When different scavengers were added, the degradation rate of dyes decreased, indicating that h^+, $\cdot O_2^-$ and ·OH all play a role in oxidative degradation. Among them, adding Na-OA reagent decreased the dye degradation rate to about 18%, which means that h^+ is the dominant active species in the photocatalytic oxidation system. Addition of t-BuOH and BQ reagents, decreased the dye degradation rate to 67% and 42%, suggesting that $\cdot O_2^-$ is also the main active species in the reaction process and ·OH has a slight effect on photodegradation.

Typically, $BiVO_4$ is an n-type semiconductor, while FeOOH is a p-type semiconductor. When these two are combined, a p-n heterojunction can be formed, which can promote the photo-generated hole-electron pairs separation (Zhang et al. 2019b). According to previous reports, the valence band potentials of $BiVO_4$ and FeOOH are 2.75 eV and 1.75 eV, respectively while the conduction band potentials of NHE are 0.30 eV and − 0.35 eV, respectively (She et al. 2020). These reasonable positions of the valence band and conduction band of the two semiconductors form type-II heterojunctions. Due to the electric field at the mass junction interface, excitons separate rapidly in this area. The photo-generated electrons migrate from the valence band of FeOOH to $BiVO_4$, the photo-generated holes are transferred from the conduction band of $BiVO_4$ to FeOOH at the same time, which significantly improves the separation efficiency of photo-generated electrons and holes. Besides, PEDOT and $BiVO_4$ form an inorganic–organic hybrid structure. Considering that the conduction band (CB) position of $BiVO_4$ is very close to the HOMO level of PEDOT, the photo-generated electrons accumulated on the

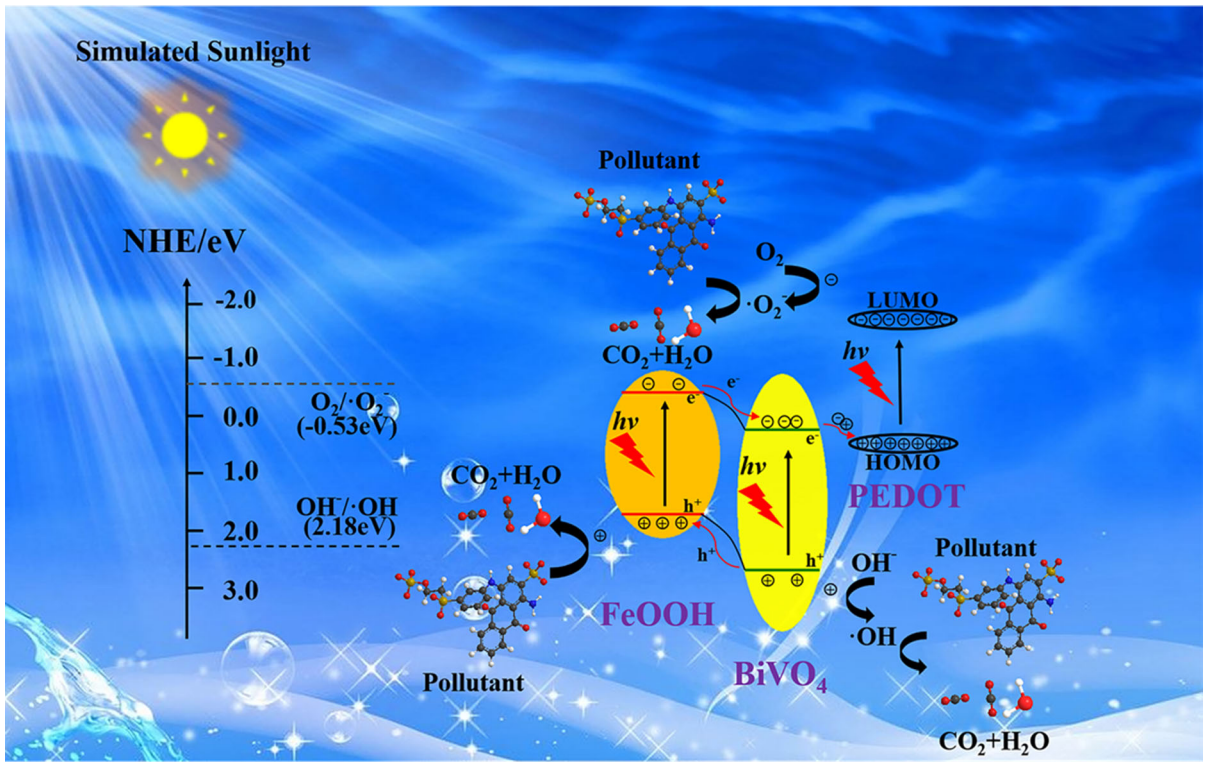

Fig. 8 The possible reaction mechanism of PEDOT/FeOOH/$BiVO_4$@Cotton in the photocatalytic degradation of pollutant (RB-19)

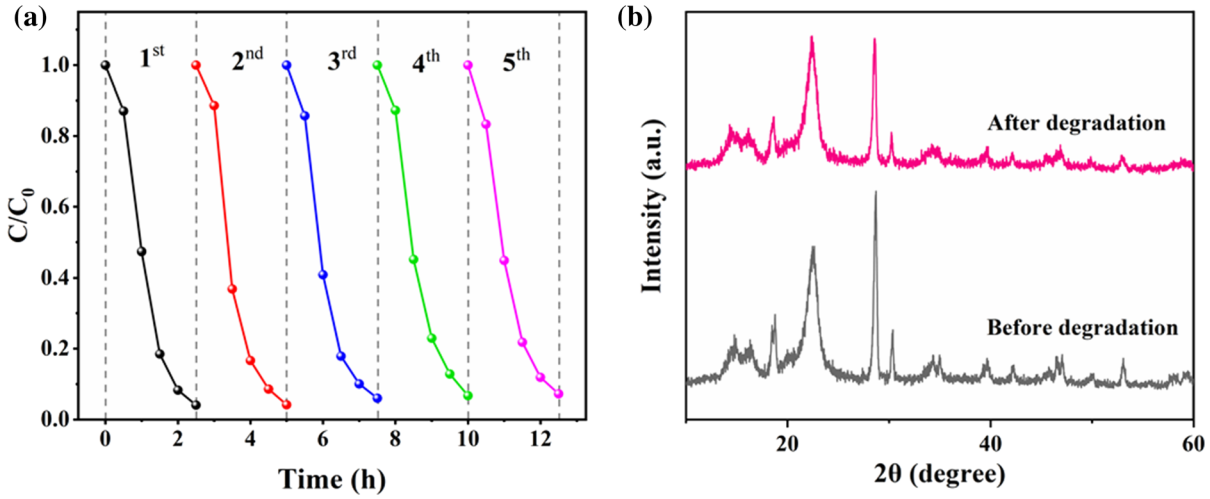

Fig. 9 The stability of the PEDOT/$BiVO_4$/FeOOH@Cotton hybrid for the photodegradation of RB-19 under light irradiation (**a**), and the XRD patterns of the corresponding sample before and after five cycles (**b**)

conduction band of $BiVO_4$ may effectively recombine with the excited-holes of HOMO (Trzciński et al. 2016). In the inorganic part, the photo-generated electron potential on LUMO is more negative than that of $O_2/\cdot O_2^-$ (− 0.53 eV), which can produce $\cdot O_2^-$, while the valence band potentials of FeOOH and $BiVO_4$ are both more positive than that of $O_2/\cdot O_2^-$ which cannot produce $\cdot O_2^-$. This is consistent with the results of free radical capture experiments.

Based on the above discussion, a potential photocatalytic mechanism of the PEDOT/$BiVO_4$/FeOOH@Cotton composite photocatalytic fabric for the efficient degradation of dyes has been proposed (Fig. 8). First, under simulated sunlight, the electrons of FeOOH and $BiVO_4$ valence band absorb energy and are excited to the conduction band, leaving positive holes. Due to the existence of the p-n heterojunction, the photoinduced electrons migrate to the conduction band of $BiVO_4$. The holes are transferred to the FeOOH valence band, and oxidation reactions occur on the surface to degrade organic pollutants. At the same time, the HOMO electrons of PEDOT are also excited to LUMO, because the position of HOMO is close to the conduction band position of $BiVO_4$. The electrons accumulated on $BiVO_4$ recombine with HOMO holes, and the photogenerated electrons with more negative potential on LUMO react with the dissolved oxygen in water to produce $\cdot O_2^-$ radicals to further mineralize organic pollutants. Although in the free radical capture experiment, the existence of a small amount of ·OH has been proven, the $OH^-/\cdot OH$ potential is 2.18 eV, only the valence band holes of $BiVO_4$ with corrected positions can oxidize OH^- to produce ·OH. This suggests that a slight excess of single $BiVO_4$ also has a certain photocatalytic effect. The possible reaction formulas in the photocatalysis process are as follows:

$$FeOOH + hv \rightarrow h_1^+ + e_1^- \quad (1)$$

$$BiVO_4 + hv \rightarrow h_2^+ + e_2^- \quad (2)$$

$$PEDOT + hv \rightarrow h_3^+ + e_3^- \quad (3)$$

$$h_2^+ + OH^- \rightarrow \cdot OH \quad (4)$$

$$\cdot OH + RB_{19} \rightarrow CO_2 + H_2O \quad (5)$$

$$h_2^+(BiVO_4) \rightarrow h_3^+(FeOOH) + RB_{19} \rightarrow CO_2 + H_2O \quad (6)$$

$$e_3^- + O_2 \rightarrow \cdot O_2^- \quad (7)$$

$$\cdot O_2^- + RB_{19} \rightarrow CO_2 + H_2O \quad (8)$$

Stability evaluation results

The stability of the composite photocatalytic fabric is critical to ensure that the fabrics can be recycled and reused. In this study, we have conducted recycling experiments to evaluate the performance of PEDOT/$BiVO_4$/FeOOH@Cotton. It is emphasized that the fabric must be cleaned with deionized water before the next cycle to ensure that most of the adsorbed dye is removed. After five cycles, we analyzed the fabric crystals before and after the degradation process. As presented in Fig. 9a, the dye photodegradation efficiency is 92.3% after the fifth cycle compared to 95.6% in the first cycle. At the same time, Fig. 9b shows the XRD patterns of PEDOT/$BiVO_4$/FeOOH@Cotton before and after photodegradation. The slight change between the two patterns further confirms the durability of the composite photocatalytic fabric and its physical stability. Besides, we have conducted washing experiments to prove the fastness of composite nanoparticles on the fabric surface. The washing method is according to the standard GB/T 3921.1–1997 in which the standard color-changing grey sample card is used to evaluate the fastness. The results showed that the fading fastness of the fabric is 4 $\sim$ 4.5, indicating that the composite nanoparticles have good fastness on the fabric surface.

Conclusions

A multi-layered photocatalytic cotton fabric can efficiently remove up to 96% of reactive dyes in wastewater under visible light. The photochemical degradation ability of the fabrics is stable and provides 92% degradation after 5 sorption-desorption cycles. A simple two-step hydrothermal process has been used to develop PEDOT/$BiVO_4$/FeOOH@Cotton fabric composite for dye remediation. Mechanism investigations show that photo-generated h^+ and $\cdot O_2^-$ are the main active species in the photocatalytic reaction process. The enhancement of photocatalytic activity can be attributed to the formation of p-n heterojunction between $BiVO_4$ and FeOOH and the rapid transfer of photo-generated electron by PEDOT, which can significantly reduce carrier recombination. No significant changes were observed in the XRD patterns of the fabric used for sorption even after 5 cycles indicating high stability. This research provides new insights for the preparation and optimization of flexible fiber substrate photocatalytic materials with visible light response. The potential applications in the field of photocatalytic environmental remediation and solar energy conversion been suggested.

Acknowledgments The authors are grateful for the financial support provided by the Fundamental Research Funds for the Central Universities (Grant No. 2232021G-04 and 2232020D-20), National Program on Key Research Project (Grant No. 2016YFC0400504) and China Postdoctoral Foundation Project (Grant No. 2017M611419).

Declarations

Conflict of interest The authors declare that they have no conflict of interest. This article does not contain studies with human participants or animals performed by any of the authors. Consent was sort from all individual participants included in the study.

References

Almeida F, Grzebielucka EC, Antunes SRM, Borges CPF, Andrade AVC, Souza ECF (2020) Visible light activated magnetic photocatalysts for water treatment. J Environ Manag 273:111143

Coelho D, Gaudêncio JPRS, Carminati SA, Ribeiro FWP, Nogueira AF, Mascaro LH (2020) Bi electrodeposition on WO_3 photoanode to improve the photoactivity of the WO_3/$BiVO_4$ heterostructure to water splitting. Chem Eng J 399:125836

Das TK, Ganguly S, Remanan S, Ghosh S, Das NC (2020) Mussel-inspired Ag/poly(norepinephrine)/MnO_2 heterogeneous nanocatalyst for efficient reduction of 4-nitrophenol and 4-nitroaniline: an alternative approach. Res Chem Intermediat 46:3629–3650

Das TK, Remanan S, Ghosh S, Ghosh SK, Das NC (2021) Efficient synthesis of catalytic active silver nanoparticles illuminated cerium oxide nanotube: a mussel inspired approach. Environ Nanotechnol Monit Manag 15:100411

Duan C, Meng X, Liu C, Ni Y (2019) Carbohydrates-rich corncobs supported metal-organic frameworks as versatile biosorbents for dye removal and microbial inactivation. Carbohyd Polym 222:115042

El-Hout SI, El-Sheikh SM, Gaber A, Shawky A, Ahmed AI (2020) Highly efficient sunlight-driven photocatalytic degradation of malachite green dye over reduced graphene oxide-supported CuS nanoparticles. J Alloy Compd 849:156573

Fan J, Yu D, Wang W, Liu B (2019) The self-assembly and formation mechanism of regenerated cellulose films for photocatalytic degradation of C.I. Reactive Blue 19. Cellulose 26:3955–3972

Gao RT, He D, Wu L, Hu K, Liu X, Su Y, Wang L (2020) Towards long-term photostability of nickel hydroxide/$BiVO_4$ photoanodes for oxygen evolution catalysts via in situ catalyst tuning. Angew Chem Int Edit 59:6213–6218

Ghosh S, Ganguly S, Remanan S, Das NC (2019) Fabrication and investigation of 3D tuned PEG/PEDOT: PSS treated conductive and durable cotton fabric for superior electrical conductivity and flexible electromagnetic interference shielding. Compos Sci Technol 181:107682

Gueye MN, Carella A, Faure-Vincent J, Demadrille R, Simonato J-P (2020) Progress in understanding structure and transport properties of PEDOT-based materials: a critical review. Prog Mater Sci 108:100616

Guo H, Li Z, Zhang Y, Jiang N, Wang H, Li J (2020) Degradation of chloramphenicol by pulsed discharge plasma with heterogeneous Fenton process using Fe_3O_4 nanocomposites. Sep Purif Technol 253:117540

He S-a et al (2020) High-efficient precious-metal-free g-C_3N_4-Fe_3O_4/β-FeOOH photocatalyst based on double-heterojunction for visible-light-driven hydrogen evolution. Appl Surf Sci 506:144948

Hu J, Li J, Cui J, An W, Liu L, Liang Y, Cui W (2020) Surface oxygen vacancies enriched FeOOH/Bi_2MoO_6 photocatalysis- fenton synergy degradation of organic pollutants. J Hazard Mater 384:121399

Ikeda S et al (2018) Effects of zirconium doping into a monoclinic scheelite $BiVO_4$ crystal on its structural, photocatalytic, and photoelectrochemical properties. Front Chem 6:266

Ivanko I, Pánek J, Svoboda J, Zhigunov A, Tomšík E (2019) Tuning the photoluminescence and anisotropic structure of PEDOT. J Mater Chem C 7:7013–7019

Ji S, Wang Q, Xu Q, Wu M, Shi W (2020) Electrospun organic/inorganic hybrid nanofibers as low-cytotoxicity and recyclable photocatalysts. Appl Surf Sci 532:147430

Ju P, Wang Y, Sun Y, Zhang D (2020) In-situ green topotactic synthesis of a novel Z-scheme Ag@$AgVO_3$/$BiVO_4$ heterostructure with highly enhanced visible-light photocatalytic activity. J Colloid Interface Sci 579:431–447

Kayser LV, Lipomi DJ (2019) Stretchable conductive polymers and composites based on PEDOT and PEDOT:PSS. Adv Mater 31:06133

Koyama T, Matsuno T, Yokoyama Y, Kishida H (2015) Photoluminescence of poly(3,4-ethylenedioxythiophene)/poly(styrenesulfonate) in the visible region. J Mater Chem C 3:8307–8310

Kumar A, Raizada P, Singh P, Saini RV, Saini AK, Hosseini-Bandegharaei A (2020) Perspective and status of polymeric graphitic carbon nitride based Z-scheme photocatalytic systems for sustainable photocatalytic water purification. Chem Eng J 391:123496

Laraib I, Carneiro MA, Janotti A (2019) Effects of doping on the crystal structure of $BiVO_4$. J Phys Chem C 123:26752–26757

Liu G, Liu S, Lu Q, Sun H, Xu F, Zhao G (2014) Synthesis of monoclinic $BiVO_4$ microribbons by sol–gel combined with electrospinning process and photocatalytic degradation performances. J Sol-Gel Sci Techn 70:24–32

Liu J, Zhang X, Xu J, Qiu J, Zhu J, Cao H, He J (2020) Anaerobic biodegradation of acetochlor by acclimated sludge and its anaerobic catabolic pathway. Sci Total Environ 748:141122

Lum PT, Foo KY, Zakaria NA, Palaniandy P (2020) Ash based nanocomposites for photocatalytic degradation of textile dye pollutants: a review. Mater Chem Phys 241:122405

Marimuthu S, Antonisamy AJ, Malayandi S, Rajendran K, Tsai PC, Pugazhendhi A, Ponnusamy VK (2020) Silver nanoparticles in dye effluent treatment: a review on synthesis, treatment methods, mechanisms, photocatalytic degradation, toxic effects and mitigation of toxicity. J Photochem Photobiol B Biol 205:111823

Park Y, McDonald KJ, Choi KS (2013) Progress in bismuth vanadate photoanodes for use in solar water oxidation. Chem Soc Rev 42:2321–2337

Ran J et al (2019) Immobilizing CuO/$BiVO_4$ nanocomposite on PDA-templated cotton fabric for visible light photocatalysis, antimicrobial activity and UV protection. Appl Surf Sci 493:1167–1176

Remanan S et al (2020) Converting polymer trash into treasure: an approach to prepare MoS_2 nanosheets decorated PVDF sponge for oil/water separation and antibacterial applications. Ind Eng Chem Res 59:20141–20154

Samadi M, Zirak M, Naseri A, Kheirabadi M, Ebrahimi M, Moshfegh AZ (2019) Design and tailoring of one-dimensional ZnO nanomaterials for photocatalytic degradation of organic dyes: a review. Res Chem Intermediat 45:2197–2254

She H, Yue P, Huang J, Wang L, Wang Q (2020) One-step hydrothermal deposition of F:FeOOH onto $BiVO_4$ photoanode for enhanced water oxidation. Chem Eng J 392:123703

Shen H, Wang M, Zhang X, Li D, Liu G, Shi W (2020) 2D/2D/3D architecture Z–scheme system for simultaneous H_2 generation and antibiotic degradation. Fuel 280:118618

Shi H, Jiang X, Chen D, Li Y, Hou C, Wang L, Shen J (2020) $BiVO_4$/FeOOH semiconductor-microbe interface for enhanced visible-light-driven biodegradation of pyridine. Water Res 187:116464

Soomro RA, Jawaid S, Kalawar NH, Tunesi M, Karakus S, Kilislioglu A, Willander M (2020) In-situ engineered MXene-TiO_2/ $BiVO_4$ hybrid as an efficient photoelectrochemical platform for sensitive detection of soluble CD44 proteins. Biosens Bioelectron 166:112439

Srinivasan A, Viraraghavan T (2010) Decolorization of dye wastewaters by biosorbents: a review. J Environ Manag 91:1915–1929

Sun G, Zhang Y, Gao Y, Han X, Yang M (2020) Removal of hard COD from biological effluent of coking wastewater using synchronized oxidation-adsorption technology: performance, mechanism, and full-scale application. Water Res 173:115517

Trzciński K, Szkoda M, Siuzdak K, Sawczak M, Lisowska-Oleksiak A (2016) Enhanced photoelectrochemical performance of inorganic–organic hybrid consisting of $BiVO_4$ and PEDOT:PSS. Appl Surf Sci 388:753–761

Wang H et al (2018) Promoting photocatalytic H_2 evolution on organic–inorganic hybrid perovskite nanocrystals by simultaneous dual-charge transportation modulation. ACS Energy Lett 4:40–47

Wang Y, Ding K, Xu R, Yu D, Wang W, Gao P, Liu B (2020a) Fabrication of $BiVO_4$/$BiPO_4$/GO composite photocatalytic material for the visible light-driven degradation. J Clean Prod 247:119108

Wang Y et al (2020b) Synthesizing Co_3O_4-$BiVO_4$/g-C_3N_4 heterojunction composites for superior photocatalytic redox activity. Sep Purif Technol 239:116562

Xue S, Xu X, Zhang L (2019) Fabrication of Ecofriendly Recycled Marimo-like Hierarchical Micronanostructure Superhydrophobic Materials for Effective and Selective Separation of Oily Pollutants from Water. Ind Eng Chem Res 58:5613–5621

Yan L, Liu B, Li W, Zhao T, Wang Y, Zhao Q (2020) Multiscale cellulosebasedself-assembly of hierarchical structure for photocatalytic degradation of organic pollutant. Cellulose 27:5241–5253

Yang R, Zhong S, Zhang L, Liu B (2020) PW_{12}/CN@Bi_2WO_6 composite photocatalyst prepared based on organic-inorganic hybrid system for removing pollutants in water. Sep Purif Technol 235:116270

Yang X et al (2021) Recent advances in photodegradation of antibiotic residues in water. Chem Eng J 405:126806

Yentür G, Dükkancı M (2020) Synthesis of Visible-Light heterostructured photocatalyst of Ag/AgCl deposited on (0 4 0) facet of monoclinic $BiVO_4$ for efficient carbamazepine photocatalytic removal. Appl Surf Sci 531:147322

Yin X et al (2019) An efficient tandem photoelectrochemical cell composed of FeOOH/TiO_2/$BiVO_4$ and Cu_2O for self-driven solar water splitting International. Int J Hydrogen Energ 44:594–604

Yu Q, Jiang L, Gao S, Zhang S, Ai T, Feng X, Wang W (2017) The highly efficient photocatalysts of B-doped ZnO microspheres synthesized on PET-ITO flexible substrate. Ceram Int 43:2864–2866

Yuan D et al (2020) All-solid-state $BiVO_4$/$ZnIn_2S_4$ Z-scheme composite with efficient charge separations for improved visible light photocatalytic organics degradation. Chinese Chem Lett 31:547–550

Zhang H, Yu D, Wang W, Gao P, Zhang L, Zhong S, Liu B (2019a) Recyclable and highly efficient photocatalytic fabric of Fe(III)@$BiVO_4$/cotton via thiol-ene click reaction with visible-light response in water. Adv Powder Technol 30:3182–3192

Zhang X, Li H, Kong W, Liu H, Fan H, Wang M (2019b) Reducing the surface recombination during light-driven water oxidation by core-shell $BiVO_4$@Ni:FeOOH. Electrochim Acta 300:77–84

Zhang G, Zhang X, Meng Y, Pan G, Ni Z, Xia S (2020a) Layered double hydroxides-based photocatalysts and visible-light driven photodegradation of organic pollutants: A review. Chem Eng J 392:123684

Zhang M, Liu Y, Zhu H, Wang X (2020b) Hierarchical bead chain $ZnFe_2O_4$-PEDOT composites with enhanced Li-ion storage properties as anode materials for lithium-ion batteries. Appl Surf Sci 529:147078